HHS Public Access

Author manuscript

Cancer Lett. Author manuscript; available in PMC 2018 April 10.

Published in final edited form as:

Cancer Lett. 2017 April 10; 391: 50–58. doi:10.1016/j.canlet.2017.01.007.

Prostaglandin E2 receptor 4 mediates renal cell carcinoma intravasation and metastasis

Yushan Zhang, **Hamsa Thayele Purayil**, **Joseph B. Black**, **Francis Fetto**, **Lauren D. Lynch**, **Jude N. Masannat**, and **Yehia Daaka**

Department of Anatomy and Cell Biology, University of Florida College of Medicine, Gainesville, FL 32610

Abstract

Treatment options for metastatic renal cell carcinoma (RCC) are limited. In this study, we investigated impact of prostaglandin E2 (PGE2) receptor 4 (EP4) on RCC metastasis. We found that knockdown of EP4 in two RCC cell lines, ACHN and SN12C, does not affect xenograft tumor take or growth rate in mice, but reduces metastasis by decreasing tumor intravasation. Using chick chorioallantoic membrane (CAM) assay, we confirmed that blockade of EP4 signaling inhibits tumor intravasation. In vitro studies associated EP4 expression and activity with RCC cell transendothelial migration (TEM). Gene expression analysis and validation assays showed that EP4 knockdown decreases expression of CD24, a ligand to the adhesion molecule P-selectin. Forced expression of CD24 in EP4 knockdown RCC rescues TEM capacity of the cells. Pharmacologic inhibition or knockdown of endothelial P-selectin blocks EP4-mediated cancer cell TEM, and inhibition of P-selectin prevents RCC tumor intravasation in CAM assay. Our results demonstrate that inhibition of EP4 attenuates the RCC intravasation and metastasis by downregulating CD24 and that P-selectin participates in tumor intravasation, implying a potential for these molecules as therapeutic targets for advanced RCC treatment.

Keywords

EP4; CD24; renal cell carcinoma; intravasation; metastasis

1. Introduction

The incidence of kidney cancer is on the rise and risk factors include behavior (tobacco smoking), environment (exposure to radiation) and hereditary conditions (inactivation of von Hippel-Lindau gene). In 2016, an estimated 62,700 Americans will be diagnosed with kidney and renal pelvis cancer and 14,240 will die from the disease [1]. The most abundant

Corresponding Author: Yehia Daaka, 1333 Center Drive, B1-005, Gainesville, FL, 32610. Phone: 352-273-8112; Fax: 352-846-1248; ydaaka@ufl.edu.

6. Conflicts of interest

None.

type of kidney cancer is renal cell carcinoma (RCC) and more than 30% of RCC patients present with locally advanced and metastatic diseases at the time of diagnosis [1]. Moreover, nearly 30% of patients with localized disease will develop tumor recurrence and metastasis after surgical removal of the primary tumor mass [2].

Metastasis remains the major cause of mortality for RCC. Drugs targeting vascular endothelial growth factor (VEGF) and mammalian target of rapamycin (mTOR) pathways are the first-line treatment options for advanced RCC. Although initially effective, these targeted therapies usually fail within a year of administration, and patient response to these drugs is variable [3]. Hence elucidation of other signaling pathways and identification of alternative therapeutic targets are in demand to address this therapeutic gap.

In metastasis, cancer cells undergo multiple transitions, including loss of cell polarity and detachment from surrounding cells in the primary tumor mass, migration and invasion through basement membrane and stromal cell layers, intravasation into the vasculature, translocation and survival in the circulation, arrest at distant organs and extravasation into the parenchyma, and micrometastasis formation and colonization in target organs [4, 5]. There are specific groups of molecules that function in concert in each step. For example, proteases are important for local invasion, whereas adhesion molecules like selectins and integrins are crucial for extravasation [6, 7].

Proinflammatory cytokine prostaglandin E2 (PGE2) is a lipid product of cyclooxygenase 2 (COX2), and both COX2 and PGE2 are overexpressed in multiple cancers [8]. Experimental evidence establishes a role for PGE2 and its G protein-coupled receptor EP4 in cancer invasion and metastasis. For example, PGE2 stimulates colorectal cancer stem cell expansion and liver metastases by activating NF-κB through EP4-MAPK and EP4-PI3K signaling [9]. PGE2-activated EP4 enhances Akt and GSK3β phosphorylation and βcatenin-TCF4-LEF1 signaling, thereby promoting lung cancer invasion and metastasis [10]. EP4-Akt signaling also upregulates the expression of CCR7 and facilitates lymphatic invasion of breast cancer [11]. In MDA-MB-231 cells, activated EP4-EGFR-ERK1/2-Egr1 pathway increases Id1 transcription and the breast cancer cell invasion [12]. We recently showed that EP4-cAMP-Epac-Rap and EP4-Akt-RGC2-RalA signal transduction cascades promote the RCC cell invasion [13, 14]. Little is known, however, about the role of EP4 in the exact steps of the metastatic cascade. The aim of this study was to reveal whether and how EP4 regulates RCC cell intravasation, thus providing rationale for targeting EP4 signaling pathway to treat metastatic RCC.

2. Materials and methods

2.1. Cell culture

Human renal cell carcinoma cell lines SN12C (National Cancer Institute) and ACHN (American Type Culture Collection) were maintained in RPMI 1640 medium (Corning) supplemented with 5% FBS (Thermo Scientific), 100 units/ml penicillin and 100 mg/ml streptomycin (Thermo Scientific). These cell lines were authenticated by STR-PCR (Genetica). HEK293T cells were maintained in DMEM medium (Corning) supplemented with 10% FBS. Neonatal human dermal microvascular endothelial cells (HMVECs; Lonza)

were grown in endothelial growth medium-2 and were used within eight passages. Cells were cultured at 37°C in a humidified 95% air, 5% CO2 atmosphere.

2.2. Gene knockdown and overexpression

For stable knockdown of EP4 gene, HEK293T cells were transfected with pLKO.1 lentiviral vector TRCN0000000204 or TRCN0000000205 (Thermo Scientific) encoding shRNAs targeting human EP4. Lentiviral supernatants were collected, and used either separately or in combination to transduce ACHN and SN12C. Lentiviral vector targeting GFP was used to establish control cells. Cells were selected with 2 μg/ml puromycin (Sigma-Aldrich) commencing 48 h after transduction to establish stable lines. Stable knockdown cells were maintained in complete medium containing 1 μg/ml puromycin. For transient knockdown of EP4 or P-selectin gene, 50 nM SMARTpool ON-TARGETplus siRNA (Dharmacon) were transfected into ACHN and SN12C cells with DharmaFECT 2 reagent (Dharmacon). To rescue CD24 expression, EP4 stable knockdown cells were transfected with pCMV6-Entry-CD24 (RC209542, Origene) or control pCMV6-Entry (PS100001, Origene) plasmid. To label cells, wild type ACHN and SN12C were transfected with GFP expressing lentiviral vector pEGIP (Addgene). Stable expressing cells were selected with 2 μg/ml puromycin.

2.3. Transendothelial migration

Transwell inserts (8 μm pore size, Corning) were coated with Matrigel (Corning; diluted 1:100) for 1 h at 37°C and then plated with 1×10^5 HMVECs. ACHN and SN12C were seeded at 5×10^4 cells/insert 24 h later. Cells were treated with EP4 selective agonist PGE1OH (Cayman), EP4 selective antagonist L161982 (Cayman), or P-selectin inhibitor KF38789 (Tocris), as indicated. The cancer cells were allowed to transmigrate for 24 h towards chemoattractant PGE1OH in 1% FBS. At termination, cells were fixed and stained with 0.1% crystal violet and those inside the insert were removed using a cotton swab. Cells migrating through the membrane were photographed and counted.

2.4. Mouse subrenal tumor implantation

All experiments involving animals were done according to protocols reviewed and approved by the Institutional Animal Care and Use Committee at the University of Florida. Male Hsd:Athymic Nude-*Foxn1*^{nu} mice (Envigo) age 6–7 weeks were grouped (n=6–7) according to body weight. Collagen (Roche) gel was prepared by mixing 2 parts of 5x RPMI 1640, pH 7.4, 1 part 10x 0.2 M HEPES, pH 7.3 and 7 parts of 3 mg/ml collagen in 0.2% acetic acid, pH 3.0. Cell pellet (1×10^6) was resuspended with collagen solution (7 μl) and incubated at 37°C for 1 h to allow gel to form. The gel containing cells was then immersed in complete culture medium overnight. Animals were anesthetized with isoflurane and left kidney was pushed out of the body cavity through a 10-mm dorsal incision. A 5-mm incision on the capsule, along the long axis of kidney, was made to form a pocket between capsule and parenchyma. Collagen gel containing cells was placed into the pocket, the kidney was eased back into the body cavity, and the opening was sutured. Tumor growth was monitored by palpation. At termination, tumor with recipient kidney, contralateral kidney, draining sentinel lymph node (SLN), lungs and liver were harvested, weighed, and fixed with 10% buffered formalin phosphate.

2.5. Immunohistochemistry (IHC)

Tumor grafts, mouse or chicken tissues, were embedded with paraffin and sectioned (6 μm). The sections were deparaffinized in xylene, rehydrated in graded alcohol, subjected to heat-induced antigen retrieval with target retrieval solution (Dako), blocked with protein block (Dako), probed with rabbit anti-human LDHA (1:100; #3582, Cell Signaling) or rabbit anti-human Ki67 (1:100; sc-15402, Santa Cruz) at 4°C overnight. Samples were washed and then incubated with SignalStainBoost IHC detection reagent (HRP, Rabbit, #8114, Cell Signaling) for 1 h. Samples were developed with AEC substrate (Dako), counterstained with hematoxylin, and mounted with faramount aqueous medium (Dako). Microscopic images were taken using a Nikon Eclipse 50i microscope equipped with a DS-Fi1 camera and NIS-elements BR3.1 software.

2.6. Metastasis assessment

Mouse SLN, liver, lung and contralateral kidney and chicken chorioallantoic membrane (CAM) sections were subjected to IHC. An organ was judged metastasis positive if at least one cancer cluster (that contained at least 2 cells) stained for both LDHA and Ki67. Metastases were quantified as metastasis incidence = number of positive organs/number of animals in that group. Experiments were repeated 3 times using SLN sections with 20 μm interval or liver, lung, kidney or CAM sections with 100 μm interval.

2.7. Chick chorioallantoic membrane (CAM) intravasation assay

In vivo intravasation was modeled by CAM assay [15–18]. Fertilized white leghorn chicken eggs (LocalHarvest) were incubated for 10 days in a rotary incubator at 38°C and relative humidity of 60%. CAM, 1 cm away from the branch point of chorioallantoic vein, was dropped by applying gentle suction created with an automatic pipette aid through a small hole made in the air sac [17, 19]. ACHN (2.5×10^6) or SN12C (1×10^6) cells in a volume of 30 μl culture medium were applied to the dropped CAM (day 0). Where indicated, developing tumors were treated daily for 6 days with KF38789 (1 mg/kg). After 7 days of stationary incubation, the primary tumors were excised and weighed, the lower CAM was cut with a cork borer (diameter 12.7 mm, Fisher), and the liver and lungs were harvested. Tissue parts were fixed in 10% buffered formalin phosphate, and kept frozen at −80°C. Primary tumors developed from GFP-labeled cancer cells were similarly harvested and mounted immediately on glass slides for fluorescence microscopic observation. The number of human cells within CAM was determined by human Alu sequence measurements using quantitative PCR and genomic DNA (30 ng) as template. Standard curve for Alu expression was generated by serial dilution of ACHN or SN12C genomic DNA mixed with CAM genomic DNA (30 ng). Gene expression was normalized to chicken GAPDH levels. Primer sequences are shown in Supplementary Table 1 [17].

2.8. Statistics

Data are expressed as mean ± SEM. Statistical analysis was performed with 1-way ANOVA with Tukey's post-test, and a $P < 0.05$ was considered statistically significant. Graphs were generated using Prism software (GraphPad) and axis labels were generated using Adobe Illustrator (Adobe).

3. Results

3.1. Knockdown of EP4 expression inhibits RCC xenograft tumor metastasis

We have previously shown that EP4 mediates PGE2-induced RCC7 and SN12C cell *in vitro* invasion [13, 14]. To investigate the role of EP4 in RCC metastasis, we stably knocked down its expression in two metastatic RCC cell lines, ACHN and SN12C. The two unique EP4 targeting shRNA lentiviruses decreased EP4 gene expression by approximately 60% (data not shown), while their combination reduced the expression in both cell lines by about 70% (Figure 1A). EP4 targeting shRNA decreased EP4 protein expression in both cell lines (Figure S1A). Given that EP4 can activate cAMP-dependent protein kinase (PKA), we used the phosphorylation of vasodilator-stimulated protein (VASP), a PKA substrate, as a surrogate indicator for EP4 expression and function [20, 21]. Knockdown of EP4 significantly reduced phosphorylation of VASP following stimulation by EP4 selective agonist PGE1OH (Figure 1B), validating the inhibition of EP4 protein expression and function by the shRNAs. These stable knockdown and control cells were implanted orthotopically into the subrenal capsule space of immunodeficient mice. Though tumor take and growth rate were similar between the two groups (Figure S1B), the sentinel lymph nodes (SLNs) from tumors with EP4 knockdown were much smaller than those of control tumors (Figure 1C). Moreover, SLN weight change (tumor draining - contralateral) was significantly less in mice harboring EP4 knockdown tumors than in controls (Figure 1D). IHC using anti-human LDHA or Ki67 antibodies further demonstrated a reduction in both metastatic lesion size and incidence in SLN, liver, lung and contralateral kidney (no metastases were found in contralateral kidney in mice with SN12C tumors), when comparing mice bearing EP4 knockdown tumors to controls (Figure 1E and 1F, Figure 2A). Ki67 had a similar staining pattern as LDHA (data not shown). Collectively, these results suggest the involvement of EP4 in RCC metastasis.

3.2. Blockade of EP4 expression inhibits cancer cell intravasation

We observed significantly smaller metastatic lesion stains immediately under the capsule of SLN for tumors with EP4 knockdown compared to controls (Figure 2A). In accordance with SLN structure and lymphatic metastasis process, cancer cells intravasated into the lymphatic capillaries will be firstly transported to the part immediately under SLN capsule [22]. As EP4 had little effect on the growth of the RCC cells that we used (Figure S1B), this observation suggests that fewer cancer cells from shEP4 tumors had intravasated into the lymphatic vessels.

We performed IHC on primary tumor xenografts and host kidneys and counted intravasation events in which tumor cells were detected in vessels outside tumor mass using Ki67 staining (Figure 2B). Blood vessels or lymphatic vessels were identified with the observation of vessel structure, endothelial cells lining, and presence of red or white blood cells. An intravasation event was determined when at least two or more Ki67 positive cell were observed to be inside a vessel (Figure 2B). We examined all the 600x fields in each section, and calculated the percentage of tumor cell intravasated vessels to the total vessels. EP4 knockdown ACHN and SN12C tumors had significantly fewer intravasated vessels compared to control (Figure 2B).

To confirm that EP4 regulates RCC cell intravasation, we performed chick chorioallantoic membrane (CAM) intravasation assay, a method used to identify and quantify intravasation. In this assay, human tumor cells are grafted onto the upper CAM, and tumor cells presented in the lower CAM are examined and quantified as an indicator of intravasation events happened in the upper CAM [15–18]. Similar to the mouse studies, EP4 exerted no impact on the size and weight of the primary tumors in CAM (Figure S1C). However, examination of cancer cells in lower CAM by IHC using anti-human LDHA (Figure 2C) showed a significant reduction in the incidence of intravasation for both ACHN and SN12C tumors with EP4 knockdown compared to controls (Figure 2D). Quantitative PCR assay amplifying human genomic Alu sequences in the lower CAM further confirmed a decrease in intravasated cancer cell numbers for EP4 knockdown tumors (Figure 2E). Taken together, these results suggest that EP4 mediates RCC tumor metastasis by regulating intravasation.

3.3. EP4 activity is associated with RCC cell TEM

We used the *in vitro* transendothelial migration (TEM) model to search for molecular mechanisms underlying the EP4-mediated RCC tumor metastasis. This model represents the processes of intravasation and extravasation by assaying the interaction between cancer cells and ECs. Briefly, human microvascular endothelial cells (HMVECs) were coated on the inner side of the membranes of transwell inserts, and cancer cells were seeded later on top of 100% confluent ECs. Under our experimental conditions, ECs did not migrate to the outside of the inserts (data not shown); therefore, all cells appearing on the outside bottom of the inserts were cancer cells that migrated across the EC layer. We treated wild type ACHN and SN12C cells with PGE1OH and observed a dose dependent increase in TEM (Figure 3A). When EP4 was knocked down with either shRNA (Figure 3B) or siRNA (Figure 3C), both ACHN and SN12C cells showed a decrease in TEM. To ascertain that the migrated cells are cancer cells only, we labeled the cancer cells with DilC12 and obtained similar results to those using the crystal violet method (Figure 3B). The knocking down of EP4 with siRNA was efficient as evidenced with the decrease in PGE1OH-induced VASP phosphorylation (Figure 3C). Furthermore, EP4 selective antagonist L161982 inhibited PGE1OH-induced VASP phosphorylation and TEM (Figure 3D) in a dose-dependent manner. These *in vitro* results showed that EP4 activity is associated with the cancer cell capacity to migrate through endothelial cell monolayer, and may explain the *in vivo* finding that EP4 mediated RCC cell metastasis by regulating intravasation.

3.4. EP4 regulates TEM via CD24

To identify EP4-regulated genes functioning in the RCC tumor metastasis, we searched the literature for genes associated with cancer cell TEM, intravasation or extravasation [6, 23, 24]. We selected 28 genes for screening using our shEP4 and control cells (Figure 4A). Eight of the genes were shown to be down-regulated significantly in both ACHN and SN12C cells with EP4 stable knockdown using quantitative PCR analysis. These genes are AKR1B10 (Aldo-keto reductase family 1 member B10), CD24 (cluster of differentiation 24), CD113 (Nectin 3), EDIL3 (EGF-like repeats and discoidin I-like domains 3), ICAM1 (intercellular adhesion molecule 1), IL8 (interleukin 8), LOX (lysyl oxidase) and PSGL1 (P-selectin glycoprotein ligand 1). These eight genes were reported to exhibit a positive correlation with TEM or extravasation [6, 23]. Functioning as ligands to P-selectin that can

be expressed on the surface of cancer cells and ECs, both CD24 and PSGL1 may participate in the direct interaction between RCC cells and vasculature ECs [25, 26]. We chose CD24 for further investigation, and could show the CD24 protein to be downregulated in EP4 knockdown cells (Figure 4B). Overexpression of CD24 (Figure 4C) rescued TEM capacity of EP4 knockdown cells (Figure 4D). These results show that CD24 mediates, at least in part, the EP4-regulated RCC cell TEM.

3.5. Endothelial P-selectin mediates TEM

Because CD24 is a ligand to P-selectin, we asked whether endothelial P-selectin may play a role in RCC cell TEM. We firstly treated cells with KF38789, a selective small molecule inhibitor of P-selectin-mediated cell adhesion [27], in TEM assay, and found that KF38789 dose-dependently inhibited TEM of wild type ACHN and SN12C cells (Figure 5A, Figure S1D). Importantly, KF38789 inhibited TEM more than regular cell migration as measured with Boyden chamber (i.e. no EC or extracellular matrix coating), suggesting that endothelial P-selectin, but not only cancer cell P-selectin, contributes to the interaction between cancer cells and ECs. To further characterize endothelial P-selectin, we knocked down its expression in HMVEC (Figure 5B). Loss of expression of P-selectin significantly blocks the TEM of both ACHN and SN12C cells (Figure 5C, Figure S1E). These results showed that endothelial P-selectin mediates the interaction between RCC cells and ECs.

3.6. Blockade of P-selectin inhibits RCC tumor intravasation

To validate that P-selectin impacts tumor intravasation, we inoculated wild type ACHN and SN12C cells into chicken upper CAM, treated the tumors with KF38789, and determined presence of cancer cells in the lower CAM by IHC staining and Alu gene expression. Results using KF38789 mirrored those with shEP4. The treatment with KF38789 did not affect tumor growth (Figure S1F) but decreased the cancer cell number in lower CAM, as evidenced by both human LDHA staining (Figure 6A) and human Alu sequence expression (Figure 6B). To further quantify the incidence of cancer cells in lower CAM, we transduced the cells with virus expressing GFP and repeated the CAM assay in the presence or absence of KF38789. At termination of the experiment, we peeled off CAMs and mounted them on slides for fluorescent cell cluster quantitation. We observed that cancer cells were invading upper CAM vessels and escaping from primary sites through the vasculature (Figure 6C a–c). Significantly more cell clusters were observed in the lower CAM vasculature in the control group compared to the KF38789 treatment group (Figure 6C d and e, and 6D). As the cells distributed and trapped in lower CAM are the evidence for intravasation, these *in vivo* results suggested that P-selectin participates in the RCC tumor intravasation, and may serve as a therapeutic target for advanced RCC.

4. Discussion

Intravasation into the blood or lymph vessels is a critical step for cancer cells to disseminate in the body. Cancer cells can enter the vasculature passively or actively, depending on cancer type, stage, genetic mutation, originating organ, mechanical stress and vascular integrity [28]. Active intravasation process may be regulated by a variety of cell types and molecules. For instance, tumor associated macrophages secrete epidermal growth factor and facilitate

breast carcinoma cells to migrate to and to intravasate into blood vessels [29]. Lymphatic ECs produce CXCL12 and CCL21, which attract cancer cells overexpressing CXCR4 or CCR7 to intravasate into lymph vessels [30, 31]. In colon cancer, interaction between Jagged1 on ECs and Dll4 on stromal cells activates Notch signaling that stimulates the cancer cell TEM and intravasation [24]. Notably, COX2 increases vascular permeability and promotes breast cancer cell intravasation [32]. In the present study, we showed that EP4 activity regulates RCC cell TEM and intravasation, potentially implicating the (COX2-) PGE2-EP4 axis in mediating RCC cell intravasation and metastasis.

CD24, a glycosyl phosphatidylinositol-anchored cell surface protein, is highly expressed in a variety of human cancer cells and is considered as a clinical biomarker for poor prognosis. CD24 can bind to cell adhesion molecules P-selectin and L1 to mediate cell-cell interaction, evoke intracellular signal pathways, and act as a driver for tumor growth and metastasis [33–35]. Accumulating evidence suggests that the COX2-PGE2-EP4 signaling pathway regulates CD24 expression. For example, in HT29 human colorectal adenocarcinoma cells, stimulation with PGE2 increases the activity of βCatenin, which in turn upregulates its direct target CD24 expression [33]. EP4 was also shown to activate GRK-βArrestin-Src-PI3K-GSK3 signaling pathway causing nuclear translocation of βCatenin that upregulated CD24 expression [36]. We showed here the downregulation of CD24 in EP4 knockdown RCC cells ACHN and SN12C. We further demonstrated that CD24 can mediate the cancer cell transendothelial migration, implying the involvement of CD24 in RCC tumor metastasis.

P-selectin is expressed on activated ECs and platelets. It plays a crucial role in the binding of circulating leukocytes to vascular ECs during the inflammatory response. It also mediates the tethering and rolling adhesion of circulating cancer cells to vasculature endothelial lining, thereby promoting cancer cell TEM, extravasation, and metastasis [25]. Here, we provided initial evidence to support the idea that endothelial P-selectin may also participate in RCC tumor intravasation.

In summary, we reported that EP4 regulates RCC cell intravasation and metastasis through regulation of CD24 expression and the possible interaction between tumor cell CD24 with endothelium P-selectin. EP4-CD24/P-selectin signaling pathway may serve as potential therapeutic target for the treatment of advanced RCC.

Supplementary Material

Refer to Web version on PubMed Central for supplementary material.

Acknowledgments

We thank Drs. Zhongzhen Nie and Prabir K. Chakraborty for technical assistance and discussion. We also thank Ms. Allyson Shea and Mr. Quais Hassan for editorial assistance. This work was supported, in part, by National Institutes of Health grant R01 CA129155.

Abbreviations

CAM chorioallantoic membrane

COX2	cyclooxygenase 2
EC	endothelial cell
EP4	E-type prostanoid receptor 4
IHC	immunohistochemistry
mTOR	mammalian target of rapamycin
PGE2	prostaglandin E2
RCC	renal cell carcinoma
SLN	sentinel lymph node
TEM	transendothelial migration
VASP	vasodilator-stimulated protein
VEGF	vascular endothelial growth factor

References

1. Siegel RL, Miller KD, Jemal A. Cancer statistics, 2016. CA Cancer J Clin. 2016; 66:7–30. [PubMed: 26742998]
2. Choueiri TK, Escudier B, Powles T, Mainwaring PN, Rini BI, Donskov F, et al. Cabozantinib versus Everolimus in Advanced Renal-Cell Carcinoma. N Engl J Med. 2015; 373:1814–1823. [PubMed: 26406150]
3. Santos N, Wenger JB, Havre P, Liu Y, Dagan R, Imanirad I, et al. Combination therapy for renal cell cancer: what are possible options? Oncology. 2011; 81:220–229. [PubMed: 22085914]
4. Talmadge JE, Fidler IJ. AACR centennial series: the biology of cancer metastasis: historical perspective. Cancer Res. 2010; 70:5649–5669. [PubMed: 20610625]
5. Valastyan S, Weinberg RA. Tumor metastasis: molecular insights and evolving paradigms. Cell. 2011; 147:275–292. [PubMed: 22000009]
6. Reymond N, d'Agua BB, Ridley AJ. Crossing the endothelial barrier during metastasis. Nat Rev Cancer. 2013; 13:858–870. [PubMed: 24263189]
7. Spano D, Heck C, De Antonellis P, Christofori G, Zollo M. Molecular networks that regulate cancer metastasis. Semin Cancer Biol. 2012; 22:234–249. [PubMed: 22484561]
8. Wang D, Dubois RN. Eicosanoids and cancer. Nat Rev Cancer. 2010; 10:181–193. [PubMed: 20168319]
9. Wang D, Fu L, Sun H, Guo L, DuBois RN. Prostaglandin E2 Promotes Colorectal Cancer Stem Cell Expansion and Metastasis in Mice. Gastroenterology. 2015; 149:1884–1895 e1884. [PubMed: 26261008]
10. Ho MY, Liang SM, Hung SW, Liang CM. MIG-7 controls COX-2/PGE2-mediated lung cancer metastasis. Cancer Res. 2013; 73:439–449. [PubMed: 23149922]
11. Pan MR, Hou MF, Chang HC, Hung WC. Cyclooxygenase-2 up-regulates CCR7 via EP2/EP4 receptor signaling pathways to enhance lymphatic invasion of breast cancer cells. J Biol Chem. 2008; 283:11155–11163. [PubMed: 18319253]
12. Subbaramaiah K, Benezra R, Hudis C, Dannenberg AJ. Cyclooxygenase-2-derived prostaglandin E2 stimulates Id-1 transcription. J Biol Chem. 2008; 283:33955–33968. [PubMed: 18842581]
13. Wu J, Zhang Y, Frilot N, Kim JI, Kim WJ, Daaka Y. Prostaglandin E2 regulates renal cell carcinoma invasion through the EP4 receptor-Rap GTPase signal transduction pathway. J Biol Chem. 2011; 286:33954–33962. [PubMed: 21832044]

14. Li Z, Zhang Y, Kim WJ, Daaka Y. PGE2 promotes renal carcinoma cell invasion through activated RalA. Oncogene. 2013; 32:1408–1415. [PubMed: 22580611]
15. Kim J, Yu W, Kovalski K, Ossowski L. Requirement for specific proteases in cancer cell intravasation as revealed by a novel semiquantitative PCR-based assay. Cell. 1998; 94:353–362. [PubMed: 9708737]
16. Quigley JP, Armstrong PB. Tumor cell intravasation alu-cidated: the chick embryo opens the window. Cell. 1998; 94:281–284. [PubMed: 9708729]
17. Zijlstra A, Mellor R, Panzarella G, Aimes RT, Hooper JD, Marchenko ND, et al. A quantitative analysis of rate-limiting steps in the metastatic cascade using human-specific real-time polymerase chain reaction. Cancer Res. 2002; 62:7083–7092. [PubMed: 12460930]
18. Juncker-Jensen A, Deryugina EI, Rimann I, Zajac E, Kupriyanova TA, Engelholm LH, et al. Tumor MMP-1 activates endothelial PAR1 to facilitate vascular intravasation and metastatic dissemination. Cancer Res. 2013; 73:4196–4211. [PubMed: 23687338]
19. Palmer TD, Lewis J, Zijlstra A. Quantitative analysis of cancer metastasis using an avian embryo model. J Vis Exp. 2011
20. Roberts W, Magwenzi S, Aburima A, Naseem KM. Thrombospondin-1 induces platelet activation through CD36-dependent inhibition of the cAMP/protein kinase A signaling cascade. Blood. 2010; 116:4297–4306. [PubMed: 20664056]
21. Zhang Y, Daaka Y. PGE2 promotes angiogenesis through EP4 and PKA Cgamma pathway. Blood. 2011; 118:5355–5364. [PubMed: 21926356]
22. Karaman S, Detmar M. Mechanisms of lymphatic metastasis. J Clin Invest. 2014; 124:922–928. [PubMed: 24590277]
23. Bauer K, Mierke C, Behrens J. Expression profiling reveals genes associated with transendothelial migration of tumor cells: a functional role for alphavbeta3 integrin. Int J Cancer. 2007; 121:1910–1918. [PubMed: 17621633]
24. Sonoshita M, Aoki M, Fuwa H, Aoki K, Hosogi H, Sakai Y, et al. Suppression of colon cancer metastasis by Aes through inhibition of Notch signaling. Cancer Cell. 2011; 19:125–137. [PubMed: 21251616]
25. Laubli H, Borsig L. Selectins promote tumor metastasis. Semin Cancer Biol. 2010; 20:169–177. [PubMed: 20452433]
26. Sagiv E, Starr A, Rozovski U, Khosravi R, Altevogt P, Wang T, et al. Targeting CD24 for treatment of colorectal and pancreatic cancer by monoclonal antibodies or small interfering RNA. Cancer Res. 2008; 68:2803–2812. [PubMed: 18413748]
27. Ohta S, Inujima Y, Abe M, Uosaki Y, Sato S, Miki I. Inhibition of P-selectin specific cell adhesion by a low molecular weight, non-carbohydrate compound, KF38789. Inflamm Res. 2001; 50:544–551. [PubMed: 11766994]
28. Bockhorn M, Jain RK, Munn LL. Active versus passive mechanisms in metastasis: do cancer cells crawl into vessels, or are they pushed? Lancet Oncol. 2007; 8:444–448. [PubMed: 17466902]
29. Wyckoff JB, Wang Y, Lin EY, Li JF, Goswami S, Stanley ER, et al. Direct visualization of macrophage-assisted tumor cell intravasation in mammary tumors. Cancer Res. 2007; 67:2649–2656. [PubMed: 17363585]
30. Muller A, Homey B, Soto H, Ge N, Catron D, Buchanan ME, et al. Involvement of chemokine receptors in breast cancer metastasis. Nature. 2001; 410:50–56. [PubMed: 11242036]
31. Perlikos F, Harrington KJ, Syrigos KN. Key molecular mechanisms in lung cancer invasion and metastasis: a comprehensive review. Crit Rev Oncol Hematol. 2013; 87:1–11. [PubMed: 23332547]
32. Gupta GP, Nguyen DX, Chiang AC, Bos PD, Kim JY, Nadal C, et al. Mediators of vascular remodelling co-opted for sequential steps in lung metastasis. Nature. 2007; 446:765–770. [PubMed: 17429393]
33. Naumov I, Zilberberg A, Shapira S, Avivi D, Kazanov D, Rosin-Arbesfeld R, et al. CD24 knockout prevents colorectal cancer in chemically induced colon carcinogenesis and in APC(Min)/CD24 double knockout transgenic mice. Int J Cancer. 2014; 135:1048–1059. [PubMed: 24500912]

34. Agarwal N, Dancik GM, Goodspeed A, Costello JC, Owens C, Duex JE, et al. GON4L Drives Cancer Growth through a YY1-Androgen Receptor-CD24 Axis. Cancer Res. 2016; 76:5175–5185. [PubMed: 27312530]

35. Sagiv E, Arber N. The novel oncogene CD24 and its arising role in the carcinogenesis of the GI tract: from research to therapy. Expert Rev Gastroenterol Hepatol. 2008; 2:125–133. [PubMed: 19072375]

36. Yokoyama U, Iwatsubo K, Umemura M, Fujita T, Ishikawa Y. The prostanoid EP4 receptor and its signaling pathway. Pharmacol Rev. 2013; 65:1010–1052. [PubMed: 23776144]

Highlights

1. Blockade of EP4 signaling inhibits RCC cell TEM, intravasation and metastasis.
2. EP4 knockdown decreases the expression of CD24.
3. Forced expression of CD24 in EP4 knockdown RCC cells rescues TEM.
4. Inhibition of P-selectin prevents RCC cell TEM and intravasation.

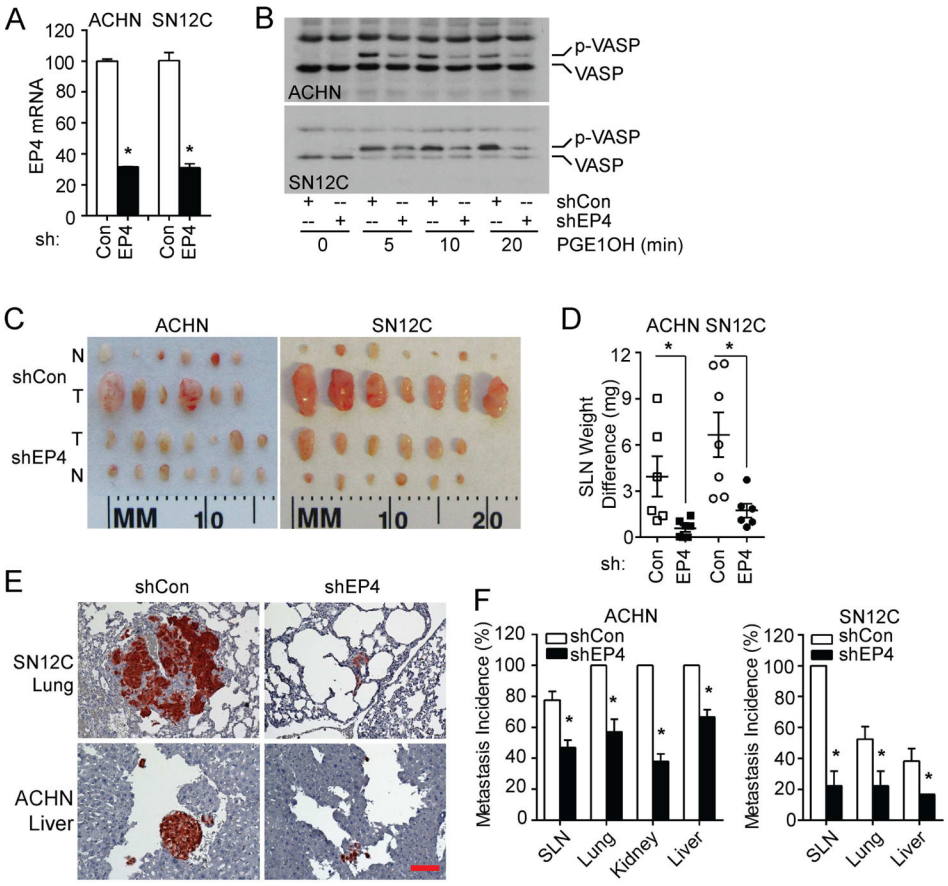

Figure 1.

Knockdown of EP4 expression inhibits ACHN and SN12C tumor metastasis. (A) ACHN and SN12C cells were transduced with shEP4 or control lentiviruses and screened to generate stable cell lines. EP4 mRNA expression was examined by quantitative PCR. (B) EP4 protein activity was verified by VASP phosphorylation, following stimulation with PGE1OH (1 μM for ACHN and 0. 1 μM for SN12C). Experiments were repeated three times with similar results. (C) 1×10^6 stable EP4 knockdown (shEP4) ACHN (n=7), SN12C (n=6) or control (shCon) ACHN (n=6), SN12C (n=7) cells were implanted under the renal capsule of athymic nude mice and allowed to grow for 8 (ACHN) or 6 (SN12C) weeks. SLNs were isolated and weighed. N, contralateral renal lymph node. T, SLN. (D) SLN weight change was calculated by subtracting weight of the contralateral renal lymph node from the weight of SLN. (E) Representative IHC staining of lung with SN12C tumor and liver with ACHN tumor by anti-human LDHA. Bar: 100 μm. (F) ACHN and SN12C tumor metastasis incidence was calculated as the number of tumor cell positive organs divided by the number of total organs in that group. Shown are the average of three experiments. *In vivo* experiments were repeated twice with similar results. For all appropriate panels, *, $P < 0.05$, vs. indicated control.

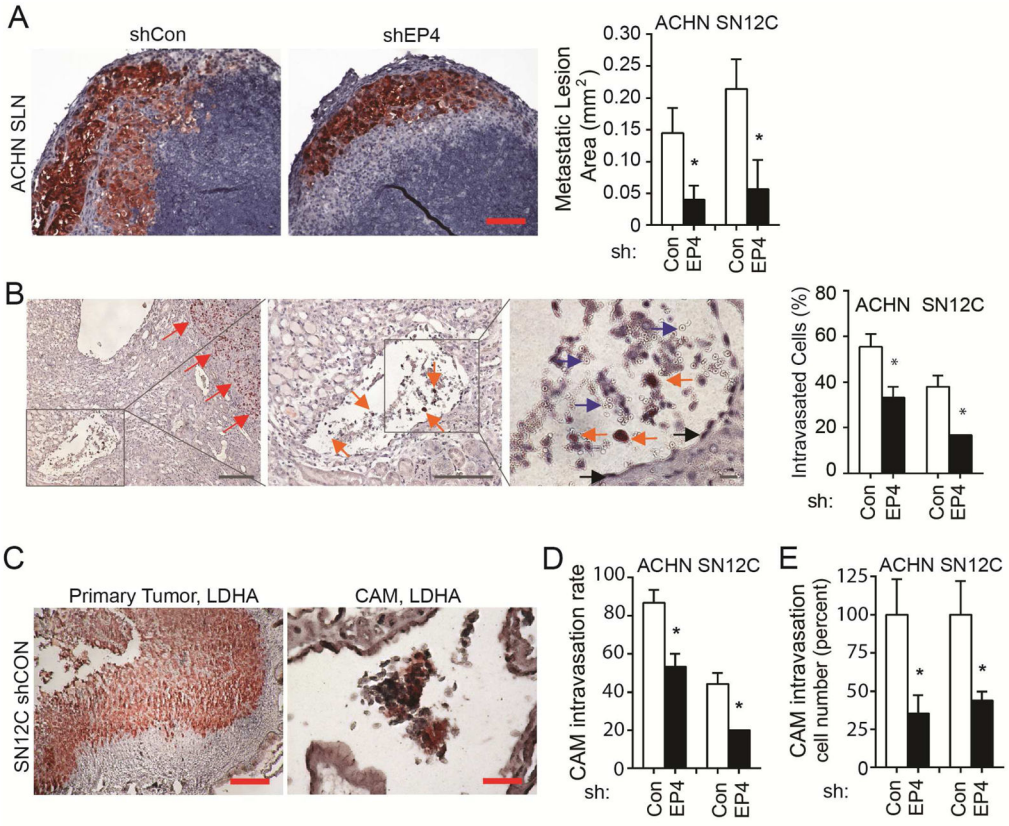

Figure 2.

Knockdown of EP4 expression inhibits ACHN and SN12C cell intravasation. (A) SLN tissues were subjected to IHC using anti-human LDHA or Ki67. Shown are typical LDHA staining from ACHN tumors, and area of metastatic lesion immediately under SLN capsule as shown by IHC. LDHA stained area was measured with Image J (graph on the right). The number of lymph nodes is indicated in Figure 1. Bar: 100 μm. (B) Typical IHC image of intravasation event in ACHN tumor xenograft in mice. Sections were stained with anti-human Ki67. Red arrow indicates primary tumor, orange arrow indicates tumor cells, blue arrow indicates red blood cells, and black arrow indicates endothelial cells. Bar: left and middle panels, 100 μm; right panel, 10 μm. Graph on the right represents all collected data. (C) Knockdown of EP4 expression inhibits ACHN and SN12C tumor cell intravasation in CAM. Cells (2.5×10^6 ACHN, 1×10^6 SN12C) with stable EP4 knockdown (shEP4) or control were inoculated on 10-day chick embryo CAMs (n=5–6 for each group) and allowed to grow for 7 days. Primary tumors and lower CAMs were subjected to IHC staining using anti-human LDHA antibody. Shown are representative IHC images of shCon-SN12C primary tumor and lower CAM. Primary tumor area and clusters of intravasated cancer cells were stained red. Bar: 200 (left) or 50 (right) μm. (D) Cancer cell intravasation rate. Intravasation rate was calculated as the number of tumor cell positive CAM divided by the number of total CAM in that group. Shown are the averages of three experiments. (E) Percent CAM intravasated cells. Lower CAM intravasated cell number relative to control was calculated based on quantitative PCR measurement of human Alu sequence expression.

CAM assays were repeated twice with similar results. All other experiments were repeated three times with similar results. For all appropriate panels, *, $P < 0.05$ vs. indicated control.

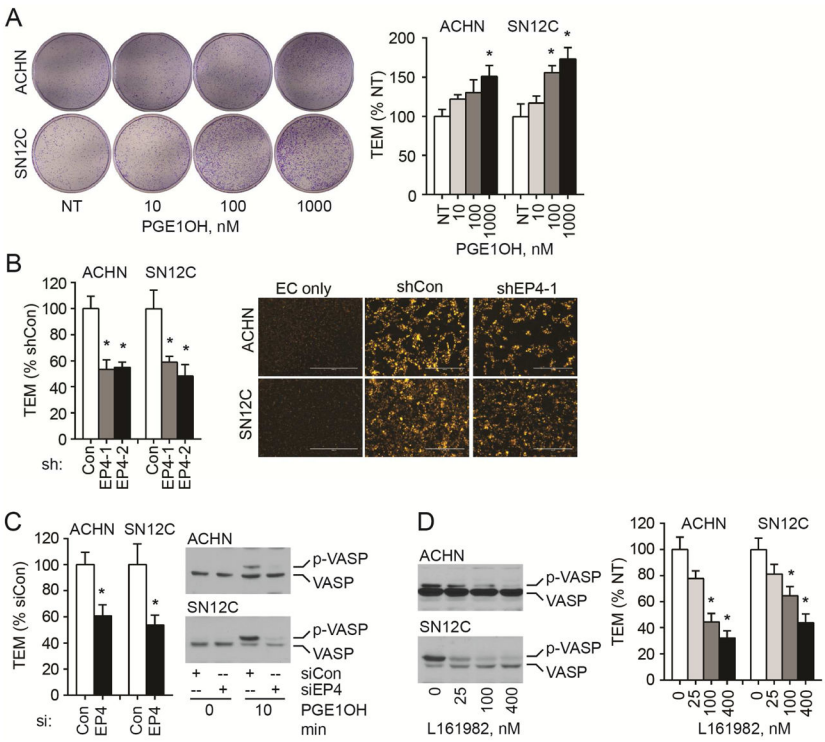

Figure 3.

EP4 expression and function are associated with RCC cell TEM in vitro. (A) Wild type ACHN and SN12C cells were treated with the indicated concentration of PGE1OH daily for three days. Cells (5×10^4) were then seeded into transwell inserts that were pre-coated with 1×10^5 HMVEC the previous day and reached 100% confluence. Cell transendothelial migration was induced by PGE1OH in 1% FBS for 24 h. Image shows the whole bottom of the insert. Cells in five 100x fields were quantitated and the ratios to not-treated cells is presented. (B) Knockdown of EP4 decreases ACHN and SN12C cell TEM. Left panel: cells with stable EP4 knockdown by two shRNA sequences (shEP4-1 and shEP4-2) were evaluated for TEM. Cell migration was induced by 1 μM (ACHN) or 0.1 μM (SN12C) PGE1OH in 1% FBS for 24 h. Right panel: ACHN and SN12C cells (shCon and shEP4-1) were labeled with DilC12 in the TEM assay. EC only; endothelial cell coated inserts without cancer cell seeding. (C) Knockdown of EP4 with siRNA attenuates TEM and EP4 signaling. TEM was examined three days after transfection and VASP phosphorylation was determined after stimulation with PGE1OH. (D) Antagonism of EP4 inhibits the PGE1OH-mediated VASP phosphorylation and TEM. Cells were treated with L161982 for 1 h and then with PGE1OH (1 μM for ACHN and 0.1 μM for SN12C), once a day for three days. All experiments were repeated three times with similar results. For all appropriate panels, *, $P < 0.05$ vs. indicated control.

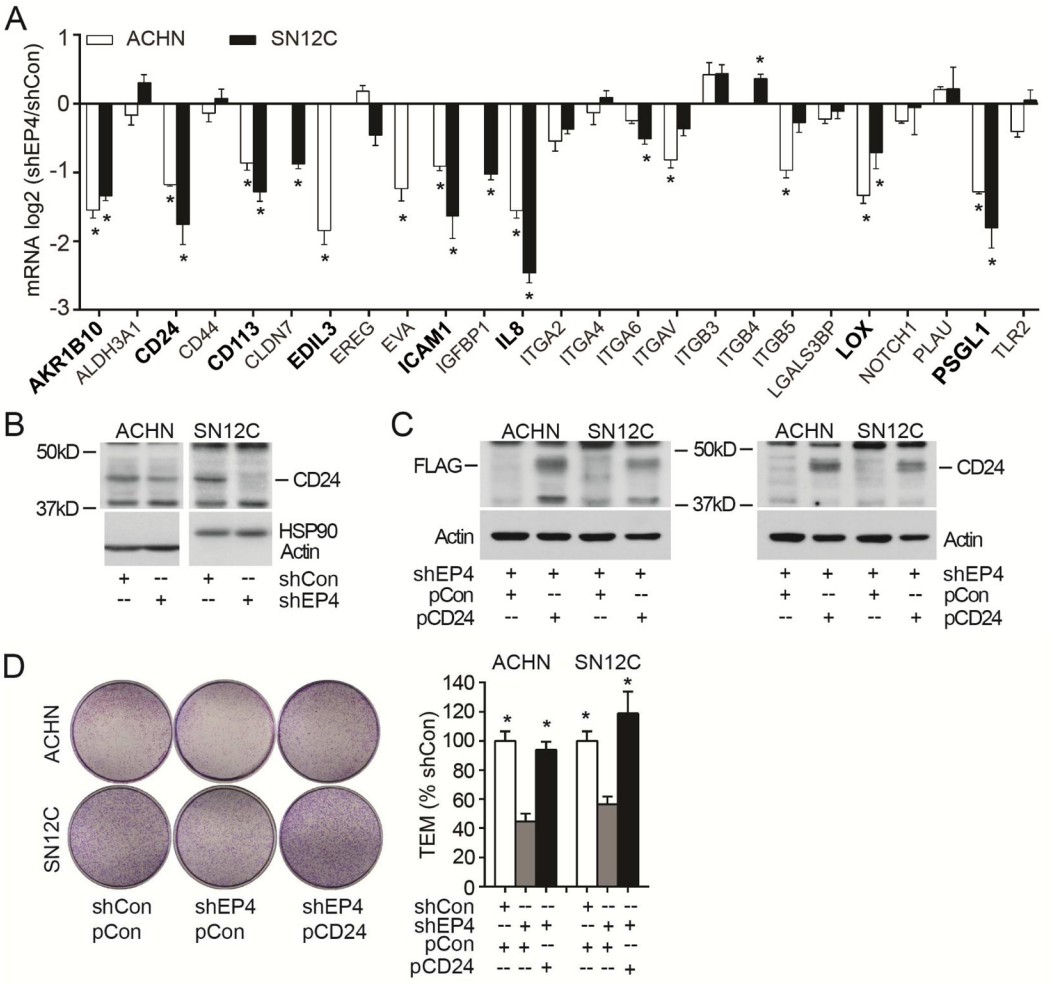

Figure 4.

EP4 regulates TEM via CD24. (A) Quantitative PCR analysis of gene expressions in EP4 knockdown ACHN, SN12C and control cells. Evaluable target genes expression is presented as the log2 value of shEP4/shCon. Depicted in bold black are genes whose expression was significantly decreased by EP4 knockdown in both ACHN and SN12C. (B) CD24 protein expression in ACHN and SN12C cells. (C) Overexpression of CD24 in EP4 knockdown cells. ACHN and SN12C cells harboring shEP4 were transfected with CD24 expressing Flag-tagged vector pCMV6-Entry-CD24 (designated as pCD24) or control vector pCMV6-Entry (as EV). Stable expression cells were selected and subjected to Western blot using Flag or CD24 antibodies. (D) Overexpression of CD24 rescues EP4 knockdown cells TEM capacity. Cells generated in (C) and shCon cells transfected with EV were used. Migrated cells in five 100x fields were counted and the ratio to shCon+EV cells is presented. All experiments were repeated three times with similar results. For all appropriate panels, *, $P < 0.05$ vs. indicated control.

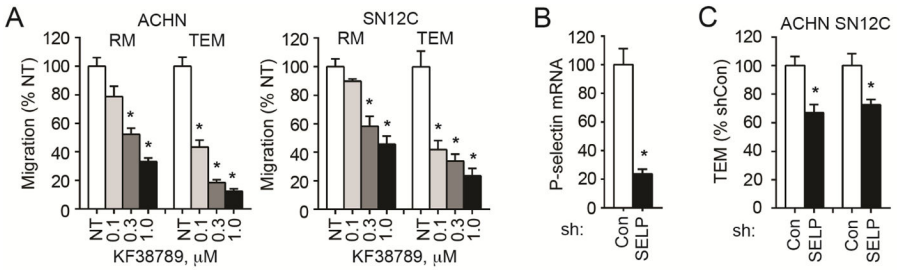

Figure 5.

Endothelial P-selection regulates RCC cell TEM. (A) KF38789 inhibits regular migration (RM) and TEM of wild type ACHN and SN12C. Cancer cells and ECs were treated with KF38789 1 h before seeding cancer cells to transwell inserts and until the end of the assay. Migration was induced by PGE1OH in 1% FBS for 24 h. Migration in five 100x fields was quantitated and is presented as the ratio to no treatment (NT). (B) Knockdown of P-selectin (SELP) in HMVEC 48 h after siRNA transfection as evidenced by quantitative PCR. (C) Knockdown of endothelial P-selectin inhibits RCC cell TEM. HMVECs (1×10^5 cells/insert) were plated 24 h after siRNA transfection and ACHN or SN12C (5×10^4 cells/insert) were seeded another 24 h later. Cancer cell migration was induced with PGE1OH in 1% FBS for 24 h. All experiments were repeated three times with similar results. For all appropriate panels, *, $P < 0.05$, vs. indicated control.

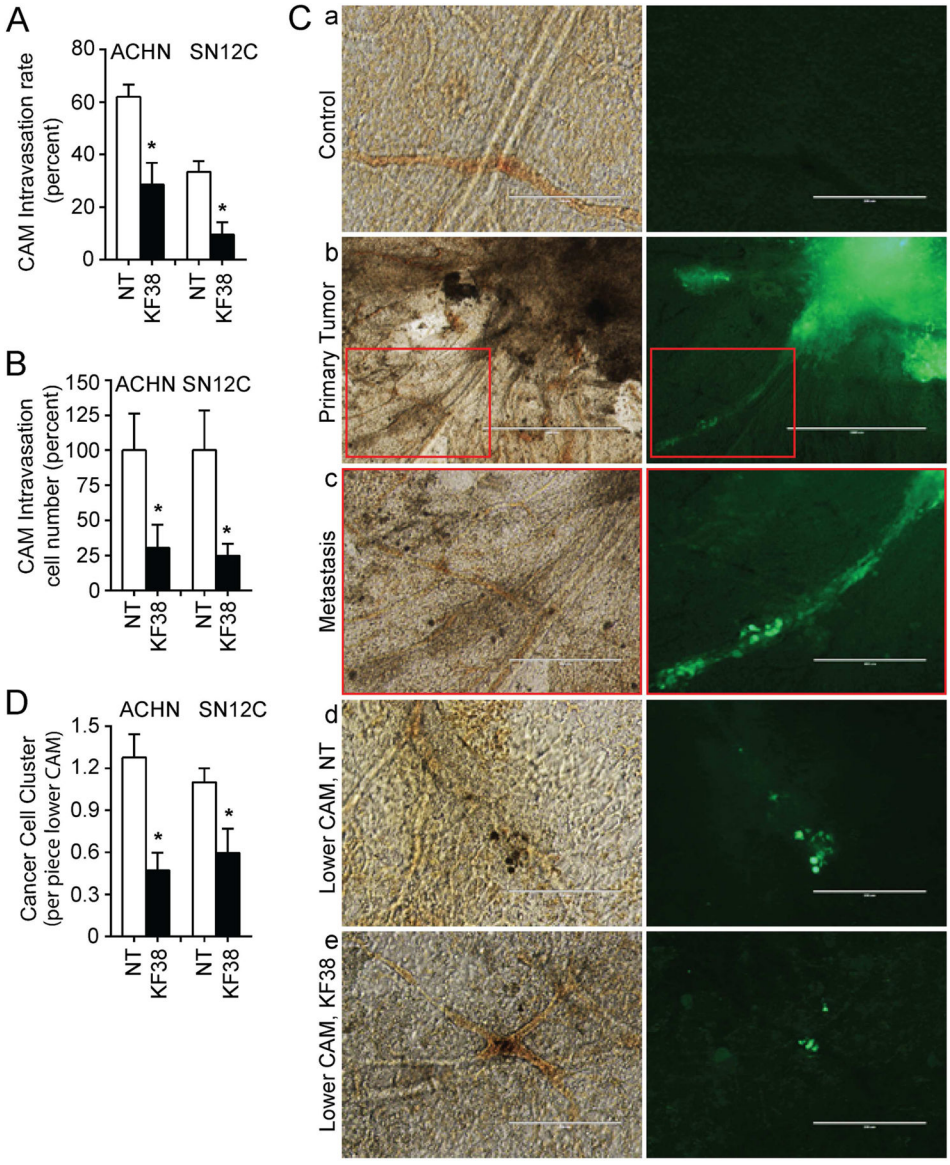

Figure 6.

Inhibition of P-selectin blocks RCC tumor intravasation. (A) ACHN (2.5×10^6) or SN12C (1×10^6) cells were inoculated on CAMs. KF38789 (KF38; 1 mg/kg egg weight) was applied directly to the tumor site daily commencing day 2 for 6 days. ACHN tumors: n=7 for both NT and treatment. SN12C tumors: n=8 for NT and n=7 for treatment. Primary tumors and organs were collected at day seven. Lower CAM sections were subjected to IHC staining using anti-human LDHA, and cancer cell intravasation rate was calculated as the number of tumor cell-positive CAMs divided by the number of total CAM in that group. Shown are the averages of three experiments. (B) CAM intravasated cell number relative to NT was calculated based on quantitative PCR analysis of human Alu sequence expression. (C) ACHN (2.5×10^6) or SN12C (1×10^6) cells expressing GFP were inoculated on CAMs (n=5–6 for each group) and treated as described in (A). Seven days after inoculation, upper CAMs with part of primary tumor, or lower CAMs cut with cork borer were mounted on

slides and observed under light or fluorescent microscopy. Images depict same light (left) and fluorescent (right) fields as follows: a, control CAM without tumor inoculation; b, primary tumor (right top corner); c, higher magnification of tumor cell invasion into vasculature shown in b red box; d, cancer cell clusters (green) in lower CAM without treatment for primary tumor; e, cancer cell clusters in lower CAM with primary tumor treated by KF38. Bar size is as follows: a, d, e, 200 μm; b, 1000 μm; and c, 400 μm. (D) Quantitation of cancer cell clusters in lower CAM. Six pieces of lower CAM from each egg were collected and cancer cell clusters were counted. For all appropriate panels, *, $P < 0.05$ vs. indicated NT.